Published in final edited form as:
*Ultrasound Med Biol*. 2010 January ; 36(1): 58–67. doi:10.1016/j.ultrasmedbio.2009.08.006.

# Molecules of various pharmacologically-relevant sizes can cross the ultrasound-induced blood-brain barrier opening *in vivo*

**James J. Choi**[*], **Shougang Wang**[*], **Yao-Sheng Tung**[*], **Barclay Morrison III**[*], and **Elisa E. Konofagou**[*,†]

[*]Department of Biomedical Engineering, Columbia University, New York, NY, USA

[†]Department of Radiology, Columbia University, New York, NY, USA

## Abstract

Focused ultrasound (FUS) is hereby shown to noninvasively and selectively deliver compounds at pharmacologically relevant molecular weights through the opened blood-brain barrier (BBB). A complete examination on the size of the FUS-induced BBB opening, the spatial distribution of the delivered agents and its dependence on the agent's molecular weight were imaged and quantified using fluorescence microscopy. BBB opening in mice ($n$=13) was achieved *in vivo* after systemic administration of microbubbles and subsequent application of pulsed FUS (frequency: 1.525 MHz, peak-rarefactional pressure *in situ*: 569 kPa) to the left murine hippocampus through the intact skin and skull. BBB-impermeant, fluorescent-tagged dextrans at three distinct molecular weights spanning over several orders of magnitude were systemically administered and acted as model therapeutic compounds. First, dextrans of 3 and 70 kDa were delivered trans-BBB while 2000 kDa dextran was not. Second, compared to 70 kDa dextran, a higher concentration of 3 kDa dextran was delivered through the opened BBB. Third, the 3 and 70 kDa dextrans were both diffusely distributed throughout the targeted brain region. However, high concentrations of 70 kDa dextran appeared more punctated throughout the targeted region. In conclusion, FUS combined with microbubbles opened the BBB sufficiently to allow passage of compounds of at least 70 kDa, but not greater than 2000 kDa, into the brain parenchyma. This noninvasive and localized BBB opening technique could thus provide a unique means for the delivery of compounds of several magnitudes of kDa that include agents with shown therapeutic promise *in vitro*, but whose *in vivo* translation has been hampered by their associated BBB impermeability.

### Keywords

Blood-brain barrier; Brain drug delivery; Focused ultrasound; FUS; HIFU; Hippocampus; Opening; Permeability; Dextran; Microbubbles



**Address Correspondence to:** Dr. Elisa E. Konofagou, Department of Biomedical Engineering, Columbia University 351 Engineering Terrace, mail code 8904 1210 Amsterdam Avenue New York, NY 10027 USA ek2191@columbia.edu Tel: 212-854-9661/212-342-0863 Fax: 212-342-5773.

## INTRODUCTION

The *in vivo* systemic delivery of neurological agents and biomarkers in the brain is critical for the induction of therapeutic effects and the understanding of biological pathways. However, most molecular targets in the brain cannot be reached due to the blood-brain barrier (BBB). Under normal conditions, the BBB provides vital physiological functions that prevent harmful toxins from entering the brain and maintain ionic and volume environments necessary for proper neuronal firing and brain function (Stewart and Tuor 1994). Unfortunately, these same properties also constitute the major impediment in delivering agents in the brain. BBB impermeability is most pronounced for molecules greater than 400 Da (Pardridge 2005) which are characteristic of the vast majority of therapeutic agents and biomarkers.

A common brain drug delivery method consists of penetrating a needle through untargeted tissue to reach a subcortical structure (Pardridge 2007). The agent diffuses the targeted region, but its spatial extent is constrained by the narrowness of the brain extracellular space (Sykova and Nicholson 2008). Alternative methods modify the chemical properties of agents to increase their trans-BBB permeability, thus utilizing the extensive capillary network. These techniques aim to increase their lipid-solubility (Greig et al. 1990), cause contraction and dilations of the vessel, or utilize transport systems endogenous to the endothelial cells (Pardridge 2007). Lipidization typically fails for larger molecules and permeability is increased throughout the entire body, thus limiting dosage due to associated side-effects. Methods that contract or dilate vessels are not localized within a specific region of the brain, and have associated toxicity. Finally, the use of endogenous transport systems requires a comprehensive knowledge of each specific agent and transport system leading to a time-consuming and costly process. Therefore, neither direct injection nor chemical modification of agents is currently sufficient as methods of brain drug delivery for many *in vivo* experiments that aim to understand neurological processes or to test the therapeutic effectiveness of drugs.

In this paper, we evaluate the potential of a novel methodology that utilizes focused ultrasound (FUS) and microbubbles to provide a noninvasive, transient, and localized technique that increases the molecular weight threshold of deliverable agents in the brain (Hynynen et al. 2001, Raymond et al. 2008). In FUS, acoustic energy propagates several centimeters through water or tissue and converges onto a small focal region (on the order of cubic millimeters) while its surroundings remain relatively unaffected. When FUS is applied, under specific acoustic parameters, in the presence of systemically administered, acoustically active, pre-formed microbubbles (<10 μm in diameter), acoustic cavitation and radiation force are induced (Apfel 1997). These bubble-ultrasound interactions have been shown to modify the BBB physiology and induce a transient influx of molecules from the lumen into the tissue parenchyma; enabling thus many previously BBB-impermeable molecules to permeate (Choi et al. 2007a, Choi et al. 2007b, Hynynen et al. 2001, Kinoshita et al. 2006, Treat et al. 2007).

Previous studies of FUS-induced BBB opening have validated the delivery of many molecules: MRI contrast agents such as Omniscan™ (573 Da) and Magnevist® (938 Da) (Choi et al. 2007a, Choi et al. 2007b, Hynynen et al. 2001), Evans Blue (Kinoshita et al. 2006), Trypan Blue (Raymond et al. 2008), Herceptin (148 kDa) (Kinoshita et al. 2006), horseradish peroxidase (40 kDa) (Sheikov et al. 2008), doxorubicin (544 Da) (Treat et al. 2007), and rabbit anti-Aβ antibodies (Raymond et al. 2008). However, the technique's potential has not been studied at length such as to be widely applicable for experiments in neuroscience. In particular, the upper limit on the molecular weight of deliverable molecules has not been determined and the spatial distribution of their delivery has not been

extensively characterized. Comparisons in efficacy of delivery amongst the aforementioned molecules are difficult since their chemical properties (i.e., charge, molecular shape, etc.) and *in vivo* circulation behavior may vastly differ or are unknown (Habgood et al. 2007). In our previous studies, we delivered 573-Da MRI contrast agents through the BBB opening, but observed that its *in vivo* spatial distribution was not Gaussian around the focus (Choi et al. 2007a, Choi et al. 2008) and was instead distributed in a heterogeneous pattern. Although we used high field (9.4T) MRI with resolution good enough (voxel size: 75×75×600 $\mu m^3$) to discern large vessels (i.e., posterior cerebral artery, longitudinal hippocampal vessels, etc.) and distinct hippocampal regions (i.e., dentate gyrus, CA1/CA2/CA3, etc.) it was not sufficient to discern smaller brain structures (i.e., hippocampal fissure, transverse hippocampal veins, cell bodies, etc.). In order to overcome the aforementioned limitations, fluorescence microscopy was employed in this study to achieve the resolution and contrast necessary to discern the spatial distribution of delivered agents relative to the underlying brain structures.

In this study, the FUS-induced BBB opening was determined using dextrans at distinct molecular weights that are relevant for biomarkers and drugs. The spatial deposition pattern of molecules in the brain was analyzed with respect to the underlying vasculature. A single delivery target, the hippocampus, was selected, since it is an anatomically distinct, subcortical structure that is perfused by an easily identifiable vasculature relative to anatomical landmarks such as the hippocampal fissure (Coyle 1975, 1976, 1978). The hippocampus is also a good target since it may be the initial site where Alzheimer's disease first manifests itself. This study will help elucidate the relevance of FUS-induced BBB opening to biomarkers and therapeutic agents used for the treatment of CNS diseases such as Alzheimer's, Parkinson's, and Huntington's disease.

## MATERIALS AND METHODS

### Ultrasound equipment

Ultrasound waves were generated by a single-element, spherical segment FUS transducer (center frequency: 1.525 MHz, focal depth: 90 mm, radius: 30 mm; Riverside Research Institute, New York, NY, USA). A pulse-echo diagnostic transducer (center frequency: 7.5 MHz, focal length: 60 mm) was aligned through a central, circular hole (radius: 11.2 mm) of the FUS transducer so that the foci of the two transducers fully overlapped (Fig. 1). A cone filled with degassed and distilled water was mounted onto the transducer system with the water contained in the cone by an acoustically transparent latex membrane cap (Trojan; Church & Dwight Co., Inc., Princeton, NJ, USA). The transducer system was attached to a computer-controlled, three-dimensional positioning system (Velmex Inc., Lachine, QC, CAN). The FUS transducer was connected to a matching circuit and was driven by a computer-controlled function generator (Agilent, Palo Alto, CA, USA) and a 50-dB power amplifier (ENI Inc., Rochester, NY, USA). The pulse-echo transducer was driven by a pulser-receiver system (Panametrics, Waltham, MA, USA) connected to a digitizer (Gage Applied Technologies, Inc., Lachine, QC, CAN) in a personal computer (PC, Dell Inc., TX, USA).

The pressure amplitudes and three-dimensional beam dimensions of the FUS transducer were measured using a needle hydrophone (needle diameter: 0.2 mm; Precision Acoustics Ltd., Dorchester, Dorset, UK) in a degassed water tank prior to the *in vivo* experiments. The pressure amplitudes reported in this paper were measured by calculating the peak-rarefactional pressure values and attenuating by 18% to correct for skull attenuation (Choi et al. 2007b). The full-width-at-half-maximum intensities of the lateral diameter and axial length of the beam were calculated to be approximately 1.32 and 13.0 mm, respectively. The

details of the calibration and skull attenuation experiments can be found in previous studies by our group (Choi et al. 2007a, Choi et al. 2007b).

### Preparation of animals

All procedures involving animals were approved by the Columbia University Institutional Animal Care and Use Committee. A total of thirteen wild-type mice (strain: C57BL/6, mass: 28 to 32 g, sex: male; Harlan, Indianapolis, IN, USA) were used in this study. The mice were anesthetized using 1.25-2.50% isoflurane (SurgiVet, Smiths Medical PM, Inc., Wisconsin, USA) throughout both the BBB opening and transcardial perfusion procedures. Between the two procedures, the mice were placed underneath a heating lamp to prevent the potential onset of hypothermia due to extended use of anesthesia.

### Blood-brain barrier opening protocol

Each mouse was anesthetized and placed prone with its head immobilized by a stereotaxic apparatus (David Kopf Instruments, Tujunga, CA, USA) (Fig. 1). The mouse hair was removed using an electric trimmer and a depilatory cream. A degassed water-filled container sealed at the bottom with thin, acoustically and optically transparent, Saran™ Wrap (SC Johnson, Racine, WI, USA) was placed on top of the mouse head while ultrasound coupling gel was used to eliminate any remaining impedance mismatch between the two surfaces (Fig. 1). The FUS transducer was then submerged in the water of the container with its beam axis perpendicular to the surface of the skull.

The focus of the transducer was positioned inside the mouse brain using a grid-positioning method that utilized the pulse-echo diagnostic transducer (Choi et al. 2007b). A grid constructed from three 0.30 mm thin metal bars with two bars parallel to one another and separated by 4.00 mm. At the center of the parallel bars a third center bar was soldered perpendicular to the two. The grid was placed in the water bath, on top of the skull, and in alignment with sutures visible through the skin. The center bar was aligned along the sagittal suture and one of the parallel bars with the lambdoid suture. A lateral two-dimensional raster-scan of the grid using the diagnostic transducer was made and the transducer's beam axis was positioned 2.25 and 2.00 mm away from the sagittal and lambdoid suture, respectively (Fig. 2a). Finally, the focal point was placed 3.00 mm beneath the top of the skull so that the acoustic wave propagated through the left parietal bone and overlapped with the left hippocampus and a small portion of the lateral region of the thalamus (Fig. 2b). The right hippocampus was not targeted and was used as the control. The grid positioning method has been previously shown to be within 0.5 mm of the target site, which was sufficiently precise to have the FUS focal spot consistently overlap with the hippocampus of the murine brain (Choi et al. 2007b).

A 25 μl bolus of ultrasound contrast agents (SonoVue®; Bracco Diagnostics, Inc., Milan, ITA) consisting of microbubbles (mean diameter: 3.0-4.5 μm, concentration: 5.0-8.0 × $10^8$ bubbles per ml) was injected into the tail vein 1 minute prior to sonication (Fig. 2). This delay of 1 min was selected since echocardiography of the mouse left ventricle validated the presence of circulating bubbles for at least 5 minutes (data not shown), and it had been previously shown to be sufficient for BBB opening across several mice (Choi et al. 2007a,Choi et al. 2008). The injected amount corresponded to a concentration of 0.78-0.89 μl/g of body mass while the clinically recommended contrast agent dosage used for B-mode imaging of cardiac chambers is 0.029 μl/g of body mass. This concentration was chosen despite the large discrepancy between these concentrations, because we were investigating a therapeutic application as opposed to a diagnostic method. We thus assumed that a higher concentration would indicate the maximum efficacy of the FUS-induced BBB opening procedure. Future experiments will be focused on reducing this bubble concentration.

Following microbubble injection, pulsed FUS (pulse rate: 10 Hz, pulse duration: 20 ms, duty cycle: 20%) was then applied at 569 kPa peak-rarefactional (mechanical index: 0.46) in a series of two intervals consisting of 30 s of sonication at a single location (i.e., the hippocampus). Between each interval, a 30-s window allowed for residual heat between pulses to dissipate and microbubbles to reperfuse the cerebral vasculature undisturbed by the acoustic wave (Choi et al. 2007a). The FUS sonication procedure was performed once and at a single location in each mouse brain.

### Fluorescent-tagged dextrans

The BBB opening was studied using five different conditions, i.e., three molecular sizes and two control cases. Approximately 10 min after FUS-induced BBB opening, the mice were intravenously injected via the femoral vein with fluorescent-tagged dextrans in three sets of distinct molecular weights of 3 ($n$=3), 70 ($n$=3), and 2000 ($n$=5) kDa. The 3 kDa and 70 kDa dextrans were tagged with Texas Red® since it provided a stronger fluorescent signal within a wavelength range that did not overlap with the autofluorescence of the murine brain. The 2000 kDa dextran were tetramethylrhodamine-tagged since they were not commercially available as conjugated to Texas Red®. In addition, two control conditions were studied with the first mouse sonicated post-microbubble injection but not injected with dextran, and the second mouse with microbubbles and 3 kDa dextran injected but without sonication.

After a 20-min wait following the dextran injection, which enabled the dextran to circulate throughout the vasculature, the mice were transcardially perfused with 30 ml of phosphate buffer saline (138 mM sodium chloride, 10 mM phosphate, pH 7.4) and 60 ml of 4% paraformaldehyde. The brain was extracted from the skull and post-fixed in paraformaldehyde overnight followed by cryoprotection in 30% sucrose overnight. The brain was embedded in optimum cutting temperature compound (Sakura Tissue-Tek O.C.T. Compound; Torrance, CA, USA), frozen in a square mold, and then serially sectioned into 300 μm slices in either a horizontal or coronal orientation using a cryostat. A 300-μm thickness was chosen since it allowed for the analysis of the arteries and veins, which were speculated to be contributing factors in drug deposition in our previous study (Choi et al. 2007a).

### Sizing of dextrans

The hydrodynamic diameter of the 3 and 70 kDa dextrans was measured using a Zetasizer (Nano-ZA, Malvern Instrument Ltd., Malvern, Worcestershire, UK) to be 2.33±0.38 and 10.2±1.4 nm, respectively. In this method, particle motion induced by laser illumination was used in the Stokes-Einstein relationship to estimate the hydrodynamic diameter. This diameter reflects that of a sphere with the same translational diffusion coefficient as that of the dextran measured. However, since the fluorescence of the markers conjugated to the dextrans interfered with the light scattering method, similar biotinylated dextrans without the fluorescent markers were sized instead for the 3 and 70 kDa dextrans. Unfortunately, unlabeled 2000 kDa dextran was not commercially available, and, therefore, a reliable measurement could not be made.

### Histological section image analysis

Bright field and fluorescent images were acquired using an inverted light and fluorescence microscope (IX-81; Olympus, Melville, NY, USA). Both Texas Red-tagged and tetramethylrhodamine-tagged dextrans were excited at 568±24 nm while emissions were filtered for 610±40 nm. For each mouse brain, three serial sections were selected at a defined cross-section of the hippocampus. Figures 3 and 4 depict an example section for each experimental setting and orientation. The following two sets of values were then quantified: the normalized increase in fluorescence in the left (targeted) hippocampus

relative to the right (untargeted) hippocampus and the area of fluorescence in the targeted hippocampus. For each section and for both cases, the hippocampus in the bright field images was manually outlined using Adobe® Photoshop® CS3 (San Jose, CA, USA) and used to isolate the hippocampus in the fluorescent images (Fig. 3G and H). The outlines did not include the PCA or longitudinal hippocampal vessels since they do not contain a BBB (Fig. 3A and B). All subsequent processing was made in MATLAB® 2007 (Natick, MA, USA). The relative increase in fluorescence was then calculated by dividing the spatially averaged fluorescence in the left hippocampus by the spatially averaged fluorescence in the right hippocampus. In order to calculate the area of fluorescence, pixels were assigned to be fluorescent if its intensity was 2.5 standard deviations above the spatially averaged right hippocampus. This threshold value was set, because it allowed for reliable and consistent fluorescence above the brain's autofluorescence. Any pixel above this threshold indicated increased fluorescence due to FUS and microbubbles. The percent area of fluorescence was then calculated by dividing the area of fluorescence by the total area of the hippocampus. The normalized increase in fluorescence and the area of fluorescence in the targeted hippocampus were averaged across three sections for each mouse brain. The values were then averaged and standard deviations were calculated for each dextran size. In the case of 3 kDa dextran, three sections for each of the three mice were analyzed for a total of nine sections processed.

### Statistical analysis

Differences between two sets of values were determined using statistical analysis. Following the calculation of the mean and standard deviation in the change of fluorescence of the left over the right hippocampus for the five sets of values, a Student's t-test was performed. The same comparison amongst the five sets of values for the increase in area of fluorescence was made. In all comparisons, a $P < 0.05$ was considered to denote a significant difference.

## RESULTS

### Trans-BBB delivery of dextrans of distinct molecular weights

All FUS-induced BBB opening procedures were performed *in vivo* in mice. Following systemic injection of SonoVue® microbubbles, FUS was delivered noninvasively through the left parietal bone and its overlying skin (Fig. 1) to a cylindrical brain tissue volume of 1.32 mm in diameter and 13.0 mm in axial length (Fig. 2A). The focal volume extended ventrally from the left parietal bone so that its axial length overlapped with the left hippocampus and part of the left lateral thalamic region (Fig. 2B). Fluorescent-tagged dextrans of 3, 70, and 2000 kDa in molecular weight were then systemically administered. Their trans-BBB delivery was then confirmed and quantified with fluorescence microscopy.

In each mouse, a horizontal or coronal section at distinct anatomical locations corresponding to those shown in Figs. 3 and 4 was analyzed. Two sets of measurements were quantified to help elucidate the extent of fluorescent markers delivered to the FUS-targeted hippocampus: the increase in spatially averaged fluorescence (Fig. 5A) and the total area of fluorescence (Fig. 5B). Two separate data sets were assumed to be different if a $P < 0.05$ was calculated with a Student's t-test.

Experiments in two control mice were performed in the cases of: (i) 3 kDa dextran injection without FUS sonication or microbubble injection and (ii) FUS sonication following microbubble injection without dextran injection. In both cases, no significant difference in the overall fluorescence was registered between the contralateral and ipsilateral hippocampi, indicating that the dextran was not BBB permeant and that neither FUS nor microbubbles induced an increase in fluorescence on their own (Fig. 5).

The average fluorescence intensity increase in the left hippocampus was determined by spatially averaging the left and right hippocampus separately and then dividing their difference by the average fluorescence in the right hippocampus. Since a spatial average was used, this calculation did not quantify how homogeneous or diffuse the fluorescence was within the outlined hippocampal region. Since we used relatively thick 300 μm sections, average autofluorescence levels were spatially homogeneous and relatively consistent among different brains (Fig. 3 D, F, H, J, and L). The mice receiving dextran of 3 kDa exhibited a high increase in average fluorescence in the sonicated hippocampus ($P < 0.05$) (Fig. 5A). Despite exhibiting a relatively lower average fluorescence compared to animals receiving the 3 kDa dextran ($P < 0.05$), animals receiving 70 kDa dextran also exhibited an increase in brain tissue fluorescence relative to the control mice ($P < 0.01$) (Fig. 5A). No significant fluorescence was observed in brain tissue after the systemic injection of 2000 kDa dextran ($P > 0.1$) in the left (targeted) hippocampus.

The percent area of the targeted hippocampus that was infused by the dextrans was also calculated for both the coronal and horizontal cross-sections. The 3 kDa and 70 kDa dextrans entered 54.2 ± 24.6% and 45.6 ± 12.6% of the targeted hippocampus, respectively. Both constituted significant increases compared to the two controls ($P < 0.05$). However, no significant difference in the total area of fluorescence could be determined ($P > 0.5$) between animals injected with 3 and 70 kDa dextrans.

## Variation in the spatial distribution of dextrans

The spatial distribution of fluorescent markers delivered across the BBB using FUS was investigated using serially sectioned brains at specific horizontal (Fig. 3) and coronal (Fig. 4) planes. In order to help elucidate the importance of the vasculature on this spatial distribution, a diagram of the vasculature within the hippocampal region adapted from Peter Coyle's artwork (Coyle 1976,1978) is depicted in Fig. 3A and B. Internal transverse hippocampal arteries, in the horizontal orientation, originated from the hippocampal fissure as indicated by the arrowhead in Fig. 3G. The vessels then arch clockwise in the region between the identifiable CA1/CA2/CA3 subfields and the Dentate Gyrus (Fig. 3A and G). Internal hippocampal veins run nearly parallel to these arteries but in the opposite direction (Fig. 3B). Multiple veins join the internal hippocampal vein, which then exits via the hippocampal fissure. The external transverse hippocampal vessels are located in the hippocampal region bordering the thalamus.

Intravenous injection of 3 kDa dextran resulted in fluorescence throughout the left hippocampus and part of its immediate surroundings (Figs. 3G, H and 4A). In particular, a greater fluorescence signal was observed near the internal and external hippocampal vessels. High levels of fluorescence were also observed along part of the lateral thalamic region bordering the hippocampus including regions surrounding the arteries and veins within the thalamus. However, in general, fluorescence was mostly distributed diffusely throughout the sonicated region.

In animals injected with 70 kDa dextran, the hippocampal regions also exhibited diffuse fluorescence (Figs. 3I, J and 4B), indicating that this dextran permeated throughout a significant portion of the hippocampus. This level of fluorescence in the diffuse region was not as high as that observed with 3 kDa dextran, but was significantly higher than the controls (Fig. 5). Qualitative analysis showed that, in addition to the diffuse fluorescence, isolated regions of higher fluorescence were distributed along the internal transverse hippocampal vessels (Fig. 3I). Higher fluorescence was also observed surrounding the vessels in the lateral thalamic region bordering the hippocampus, similar to the 3 kDa dextran.

No significant fluorescence was observed in the left hippocampus after injection of 2000 kDa dextran (Fig. 5A). However, outside the hippocampal region, fluorescence was qualitatively observed along the left longitudinal hippocampal vessels, the PCA, and the immediate branches originating from the two (Figs. 3K, L and 4C).

All of the aforementioned results strongly indicated not only the size of the BBB opening and the spatial distribution of dextran according to its molecular weight, but also a correlation between the spatial distribution of dextran and the location of vessels.

## DISCUSSION

This study elucidates the relevance of FUS-induced BBB opening as a method for understanding biological processes and for testing the therapeutic effectiveness of drugs. Our method neither requires an MRI system, nor a craniotomy. It is spatially accurate, and is simple enough to implement in most laboratories. A single, one-minute FUS application combined with microbubbles was sufficient to noninvasively and selectively open the BBB and deliver molecules larger than the BBB's natural size exclusion threshold of 400 Da. As our model tracers, we chose 3, 70, and 2000 kDa dextrans that were fluorescently tagged. The 3 and 70 kDa dextrans were measured by dynamic light scattering to have a hydrodynamic diameter of 2.33±0.38 and 10.2±1.4 nm, respectively. In one study, 3 and 70 kDa dextrans were found to be 3 and 14 nm in diameter (Thorne and Nicholson 2006), and, in another, the 70 and 2000 kDa dextrans were found to be 14.8 and 54.4 nm in diameter, respectively (Lebrun and Junter 1994).

This study has determined that the molecular weight threshold for dextran traversing the FUS-induced BBB opening was between 70 and 2000 kDa and that the 2000 kDa dextran could not be delivered. This suggests that there is a size limit associated with the technique. Large molecules and other constituents within the circulatory system, such as microbubbles (1-10 μm) and red blood cells (8 μm), cannot cross the FUS-opened BBB. According to prior literature, the largest molecule delivered through using FUS was Herceptin at 148 kDa (Kinoshita et al. 2006), which is within the threshold range reported here. Despite the fact that Herceptin has different chemical properties than dextran, it may suggest that the molecular weight threshold, beyond which a molecule cannot be delivered via the FUS-induced BBB opening, may lie between 148 and 2000 kDa.

Both 3 and 70 kDa dextrans were shown to traverse the BBB after 1-min FUS sonication at a single location (i.e., onto the hippocampus) by an increase in the fluorescence throughout the targeted region (Figs. 3G-H and 5B). When comparing these two molecules, the 3 kDa dextran was distributed throughout the sonicated hippocampus at a higher overall relative concentration (Fig. 5). The 70 kDa dextran was spatially distributed in two distinct patterns: a low level of fluorescence that was diffuse throughout the hippocampus, and high levels of fluorescence consisting of punctated regions near, or along, larger vessels such as the internal and external transverse hippocampal vessels, the longitudinal hippocampal artery, and the PCA. In the case of the punctate regions, fluorescence did not extend further than a few microns away. The 70 kDa dextran also accumulated along the longitudinal hippocampal arterial wall, suggesting that the markers were either contained within, or attached to, the membranes of cells that constitute the vascular wall such as endothelial and smooth muscle cells (Fig. 4B). Both 3 and 70 kDa dextrans were most concentrated at or near the internal and external hippocampal vessels and the vessels within the thalamus (Figs. 3B, I and 4A, B).

In order to determine what proportion of the hippocampus could be treated and whether the permeated area would vary with the molecular weight of the molecules delivered, the

percent area of the hippocampus exhibiting fluorescence was calculated. Dextrans were delivered to a significant percentage of the total targeted area (i.e., hippocampus): 54.2 ± 24.6% for 3 kDa dextran and 45.6 ± 12.6% for 70 kDa dextran in the cross-section analyzed (Fig. 5B). The center of the acoustic focal volume (i.e., the focal point) was positioned to overlap with the medial portion of the hippocampus and avoid overlap of the beamwidth with the lateral side of the skull. This placement away from the lateral hippocampal region limited the spatial extent of the BBB opening to the hippocampus. In future studies, a larger, or smaller, area of BBB opening could be induced by adjusting the pressure amplitude, altering the FUS transducer geometry, or sonicating multiple locations.

The acoustic parameters and microbubbles described in this study have been used in many of our previous and concurrent experiments. The spatial deposition patterns of 3 kDa dextran (Fig. 6B) obtained in this study correlated with our previous high-field $T_1$-weighted spin-echo MRI study (Fig. 6A) (Choi et al. 2008) that quantified the *in vivo* deposition of a 573-Da MRI contrast agent (gadolinium) through the FUS-induced BBB opening of separate mice (Choi et al. 2007a). Similar to the results shown in Figs. 3 and 4, the gadolinium molecules accumulated in the parenchyma through the FUS-induced BBB opening. However, they were distributed in a non-gaussian and heterogeneous pattern (Fig. 6A). This observation helped contribute to the rationale for performing the present study. Preliminary assessment of the safety of FUS-induced BBB opening using the same acoustic parameters reported in this paper is part of a concurrent study. Hematoxylin and eosin-stained sections of FUS-induced BBB opened brains revealed petechial red blood cell extravasations, but no neuronal damage (Konofagou et al. 2009). The *in vivo* assessment of the spatial distribution of MRI contrast agents and the comprehensive assessment of safety are some of our ongoing studies that, together with the results from this paper, will help elucidate the greater potential of FUS-induced BBB opening.

Four major findings were reported in this paper. First, dextrans of 3 and 70 kDa were delivered trans-BBB while 2000 kDa dextran was not. Second, compared to 70 kDa dextran, a higher concentration of 3 kDa dextran was delivered through the opened BBB. Third, the 3 and 70 kDa dextrans were both diffusely distributed throughout the targeted brain region. However, the 70 kDa dextran was diffuse at a lower concentration while having numerous punctate regions of higher concentration, indicating a more heterogeneous overall distribution. Finally, dextrans were deposited at larger amounts proximal to larger vessel branches such as the internal and external transverse hippocampal vessels, and the vessels within the thalamus, when compared to other regions in the targeted hippocampus. These results suggest that FUS and microbubbles may deliver 70 kDa agents across the BBB, but that 3 kDa and smaller agents may be delivered at a more effective concentration. A broader applicability for delivering inhibitors, growth factors, peptides, and other biomarkers and therapeutic agents to a volume on the order of cubic millimeters was thus shown. FUS and microbubbles constitute a non-contact, noninvasive, localized, and transient delivery method for cortical and subcortical structures with the critical capability of depositing agents at sizes relevant for biomarkers and neurologically potent drugs.

## Acknowledgments

This study was supported by NSF CAREER 0644713 and NIH R21 EY018505. We especially wish to thank the Riverside Research Institute (New York, NY, USA) for providing the transducers, Kenneth Hess and Fan Hua (Department of Neurology, Columbia University, New York, NY, USA) for animal assistance and training, Sujan Doshi and Abhiraj Modi for assistance with the *in vivo* mouse experiments, Kristen Kim for tracing the hippocampus, and Melissa Simon (Department of Biomedical Engineering, Columbia University, New York, NY, USA) for consultation with fluorescence imaging and sectioning procedures.

## REFERENCES


Apfel RE. Sonic effervescence: A tutorial on acoustic cavitation. Journal of the Acoustical Society of America 1997;101:1227–37.

Choi JJ, Pernot M, Brown TR, Small SA, Konofagou EE. Spatio-temporal analysis of molecular delivery through the blood-brain barrier using focused ultrasound. Phys Med Biol 2007a;52:5509–30. [PubMed: 17804879]

Choi JJ, Pernot M, Small SA, Konofagou EE. Noninvasive, transcranial and localized opening of the blood-brain barrier using focused ultrasound in mice. Ultrasound Med Biol 2007b;33:95–104. [PubMed: 17189051]

Choi JJ, Wang S, Brown TR, Small SA, Duff KE, Konofagou EE. Noninvasive and transient blood-brain barrier opening in the hippocampus of Alzheimer's double transgenic mice using focused ultrasound. Ultrasonic Imaging 2008;30:189–200. [PubMed: 19149463]

Coyle P. Arterial patterns of the rat rhinencephalon and related structures. Exp Neurol 1975;49:671–90. [PubMed: 1204702]

Coyle P. Vascular patterns of the rat hippocampal formation. Exp Neurol 1976;52:447–58. [PubMed: 954917]

Coyle P. Spatial features of the rat hippocampal vascular system. Exp Neurol 1978;58:549–61. [PubMed: 620709]

Greig NH, Daly EM, Sweeney DJ, Rapoport SI. Pharmacokinetics of chlorambucil-tertiary butyl ester, a lipophilic chlorambucil derivative that achieves and maintains high concentrations in brain. Cancer Chemother Pharmacol 1990;25:320–5. [PubMed: 2306791]

Habgood MD, Bye N, Dziegielewska KM, Ek CJ, Lane MA, Potter A, Morganti-Kossmann C, Saunders NR. Changes in blood-brain barrier permeability to large and small molecules following traumatic brain injury in mice. Eur J Neurosci 2007;25:231–8. [PubMed: 17241284]

Hynynen K, McDannold N, Vykhodtseva N, Jolesz FA. Noninvasive MR imaging-guided focal opening of the blood-brain barrier in rabbits. Radiology 2001;220:640–6. [PubMed: 11526261]

Kinoshita M, McDannold N, Jolesz FA, Hynynen K. Noninvasive localized delivery of Herceptin to the mouse brain by MRI-guided focused ultrasound-induced blood-brain barrier disruption. Proc Natl Acad Sci U S A 2006;103:11719–23. [PubMed: 16868082]

Konofagou, EE.; Choi, JJ.; Baseri, B.; Lee, A. Characterization and Optimization of Trans-Blood-Brain Barrier Diffusion In Vivo. In: Ebbini, ES., editor. 8th International Symposium on Therapeutic Ultrasound: AIP; 2009. p. 418-22.

Lebrun L, Junter GA. Diffusion of Dextran through Microporous Membrane Filters. Journal of Membrane Science 1994;88:253–61.

Pardridge WM. The blood-brain barrier: bottleneck in brain drug development. NeuroRx 2005:3–14. [PubMed: 15717053]

Pardridge WM. Drug targeting to the brain. Pharmaceutical research 2007;24:1733–44. [PubMed: 17554607]

Raymond SB, Treat LH, Dewey JD, McDannold NJ, Hynynen K, Bacskai BJ. Ultrasound enhanced delivery of molecular imaging and therapeutic agents in Alzheimer's disease mouse models. PLoS ONE 2008;3:e2175. [PubMed: 18478109]

Sheikov N, McDannold N, Sharma S, Hynynen K. Effect of focused ultrasound applied with an ultrasound contrast agent on the tight junctional integrity of the brain microvascular endothelium. Ultrasound Med Biol 2008;34:1093–104. [PubMed: 18378064]

Stewart PA, Tuor UI. Blood-eye barriers in the rat: correlation of ultrastructure with function. The Journal of comparative neurology 1994;340:566–76. [PubMed: 8006217]

Sykova E, Nicholson C. Diffusion in brain extracellular space. Physiol Rev 2008;88:1277–340. [PubMed: 18923183]

Thorne RG, Nicholson C. In vivo diffusion analysis with quantum dots and dextrans predicts the width of brain extracellular space. Proc Natl Acad Sci U S A 2006;103:5567–72. [PubMed: 16567637]

Treat LH, McDannold N, Vykhodtseva N, Zhang Y, Tam K, Hynynen K. Targeted delivery of doxorubicin to the rat brain at therapeutic levels using MRI-guided focused ultrasound. International journal of cancer 2007;121:901–7.

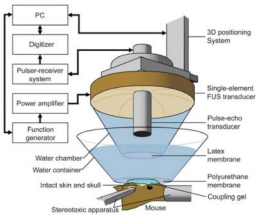


**Fig. 1.**

*In vivo* FUS-induced BBB opening experimental setup. The hair on the mouse head was removed and its head was stabilized using a stereotaxic apparatus. The single-element FUS transducer was used to induce localized BBB opening through the intact skin and skull and was driven by a PC-controlled function generator through a power amplifier. The pulse-echo transducer was used for targeting the hippocampus of the mouse brain (Fig. 2) and was triggered by a pulser-receiver system whose data was collected with a digitizer in a PC. Ultrasound was coupled to the mouse head via a water chamber and container while the ultrasound system was positioned with a three-dimensional positioning system.

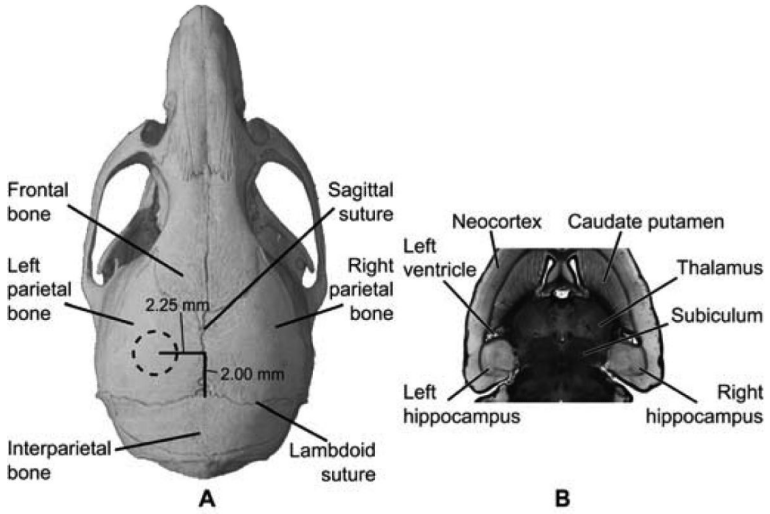


**Fig. 2.**

Location of FUS-targeted regions *in vivo*. The FUS transducer was targeted through (A) the left parietal bone of the mouse skull. The dotted circle in (*A*) approximately corresponds to the 1.32 mm full-width-at-half-maximum peak diameter of the focus. The focal volume was placed to overlap the left hippocampal region as seen on a horizontal histological section (B) of the mouse brain. The right hippocampal region was not targeted and acted as a control.

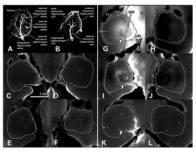

**Fig. 3.**

Horizontal sections (300 μm thick) of the left (targeted; C, E, G, I, K) and right (untargeted; D, F, H, J, L) hippocampal regions of five mouse brains. The area within the dashed white lines was defined as the hippocampal region. The hippocampal vasculature is depicted in (A) for arteries and (B) for veins roughly corresponding to the horizontal sections depicted. The diagrams were adapted from Peter Coyle's artwork (Coyle 1976, 1978). Anatomical regions were labeled in (G): left ventricle (LV), thalamus (Th), CA1, CA2, CA3, dentate gyrus (DG), posterior cerebral artery (pca), and longitudinal hippocampal artery (lha). It should be noted that the pca and lha were not within the hippocampal region (A, B, and G) and were intentionally excluded since they are not part of the hippocampus. The hippocampal fissure indicated by the arrows is where the transverse hippocampal vessels enter and exit the hippocampus. The first mouse (C, D) was injected with 3 kDa fluorescent-tagged dextran, but no sonication was applied. The second mouse (E, F) was sonicated, but no dextran was injected. In these two mice, no significant difference in fluorescence between the contralateral hippocampal regions was observed. Fluorescence was observed in the targeted hippocampal region when 3 kDa (G, H) and 70 kDA (I, J) dextrans were injected after sonication. The 3 and 70 kDa dextrans permeated 54.2 ± 24.6% and 45.6 ± 12.6% of the targeted hippocampus area, respectively (Fig. 5B). No difference in fluorescence was observed in the left hippocampal region of mice injected with 2000 kDa (K, L) dextran when compared to the right.

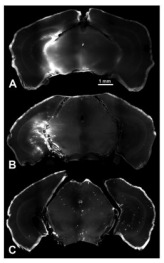


**Fig. 4.**

Coronal sections (300 μm thick) of the hippocampi of three mouse brains. Fluorescence was observed in the targeted hippocampus when 3 kDa (A), and 70 kDa (B) dextrans were injected after sonication. No significant fluorescence was observed after 2000 kDa (C) dextran was injected after sonication.

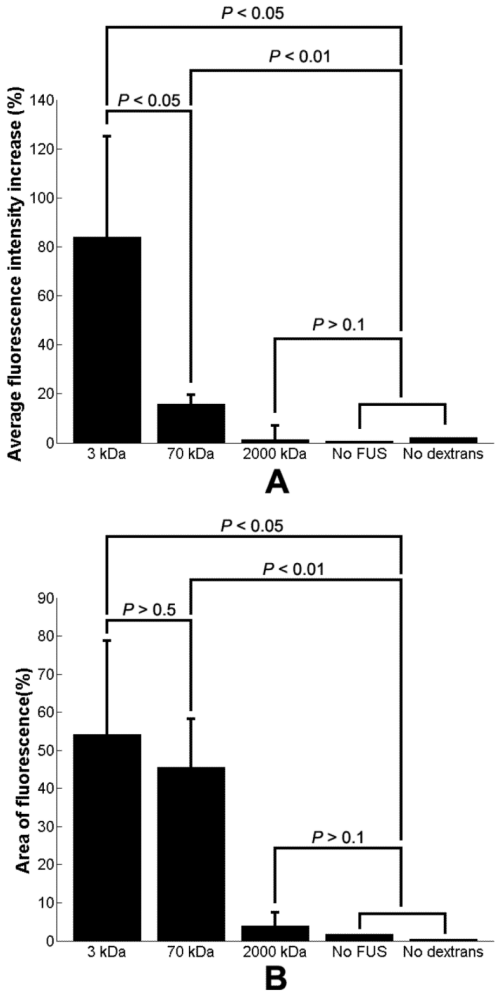


**Fig. 5.**

(A) The normalized increase in the spatially averaged fluorescence of the left (targeted) hippocampus over the right (untargeted) hippocampus. Sonication after intravenous injection resulted in increased fluorescence in the targeted hippocampus for 3 kDa and, to a lesser extent, 70 kDa dextran. No significant fluorescence was observed after 2000 kDa dextran was injected. In two controls, where dextran was injected but no sonication was applied, and where sonication was applied but no dextran was injected, almost no increase in fluorescence compared to the contralateral side was observed. (B) An increase in the percent area of fluorescence was also observed in both the case of 3 kDa and 70 kDa dextran administration without any significant difference between the two. No increase in area of fluorescence compared to the control was observed after injection of 2000 kDa dextran.

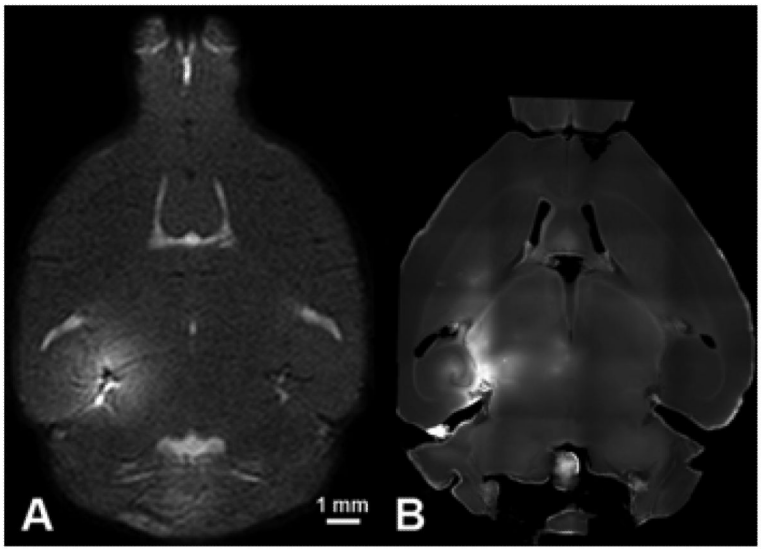


**Fig. 6.**

Comparison of results obtained using MRI and fluorescence microscopy. (A) MR images acquired on the same day as BBB opening reveal MR contrast agent (574 Da) leakage throughout the left (targeted) hippocampus and the surrounding regions. (B) In the same mouse, at 24h post-sonication, a second injection of MR contrast agent and MR imaging revealed that the BBB had closed (i.e., no leakage of the contrast agent). The spatial extent of BBB opening on the MR image in (A) is in good agreement with the (C) BBB opening indicated by injection of 3 kDa fluorescent-tagged dextrans.